Surface Acidity and Properties of Titania–Silica Catalysts

Mercedes Galán-Fereres,[†] Luís J. Alemany,[†] Rafael Mariscal,[†] Miguel A. Bañares,[†] James A. Anderson,[‡] and José L. G. Fierro*,[†]

Instituto de Catálisis y Petroleoquímica, C.S.I.C., Campus UAM, Cantoblanco E-28049-Madrid, Spain, and Department of Chemistry, The University, Dundee DD1 4HN, Scotland, U.K.

Received January 27, 1995. Revised Manuscript Received April 26, 1995[⊗]

Titania-coated silica microspheres containing between 8 and 48 wt % TiO_2 have been prepared by the homogeneous precipitation of $TiCl_3$ with a diluted ammonia solution up to a final pH close to 7. All these TiO_2–SiO_2 materials were physically characterized by X-ray diffraction, UV–visible reflectance, Raman, Fourier transform infrared, and photoelectron spectroscopic techniques. Calcination of the silica-supported precipitates leads to the formation of titanium dioxide. These TiO_2 species are scattered on the surface as small crystals of anatase. Their structures become better defined as the titania loading increases. It was also observed that the TiO_2–SiO_2 oxides show much stronger acidic properties than the single TiO_2 and SiO_2 oxides. Brönsted acid sites appear to be associated with the interface between octahedral titanium sites and silica. The infrared spectra of chemisorbed ammonia was very useful to charaterize acid properties in these materials.

Introduction

Titania-supported redox oxides constitute one of the most important categories of catalysts for the selective catalytic reduction (SCR) of NO_x.[1-7] The use of bulk titania, however, presents serious drawbacks. Commercial titania is expensive, is rather difficult to extrude to mechanically strong bodies, and has a relatively low surface area compared with the conventional silica or alumina supports. However, neither silica nor alumina can replace titania as support for the SCR catalysts. As vanadia interacts very weakly with silica,[8,9] it tends to agglomerate leading to a reduction in vanadia exposure and poorer catalytic performance.[10] On the other hand, vanadia supported on alumina is not resistant enough to poisoning by sulfur dioxide.[11] Accordingly, to avoid these deficiencies, composite supports containing titania deposited on silica or alumina have been attempted in recent years.[12-20]

Titania–silicas display unusual physical properties not only for advanced materials but also for catalytic purposes.[19,21-24] It has long been observed that certain mixed oxides show much stronger acidic properties than the single oxides of which they are composed. Examples are SiO_2–MO_x (MO_x = Al_2O_3, ZrO_2, MgO, and TiO_2). The mechanism of the generation of acidity results of chemically mixing oxides has been the subject of many studies. This acidity has been generally considered to result from an excess negative or positive charge caused by the formation of nonequivalent bridged heterometal–oxygen (Si–O–M).[5,21] The preparation of TiO_2–SiO_2 often involves hydrolysis of solutions of an alkyl silicate and alkyl titanate. Addition of an alkali metal results in quick hydrolysis and condensation–polymerization reactions of one of the precursors, starting at pH values as low as 1–2. To avoid this, the methodology employed in the present work involved the homogeneous precipitation of titanium,[7] by hydrolysis of a $TiCl_3$ solution,

[†] Instituto de Catálisis y Petroleoquímica.
[‡] The University.
[⊗] Abstract published in *Advance ACS Abstracts,* June 1, 1995.

(1) Yaverbaum, L. H. *Nitrogen Oxides Control and Removal: Recent Developments*; Noyes Data Co.: Park Ridge, NJ, 1979.
(2) Inomata, M.; Miyamoto, A.; Murakami, Y. *J. Catal.* **1980**, *62*, 140.
(3) Morikawa, S.; Takahashi, K.; Mogi, J.; Kurita, S. *Bull. Chem. Soc. Jpn.* **1982**, *55*, 2254.
(4) Yoshida, H.; Takahashi, K.; Sekiya, Y.; Morikawa, S.; Kurita, S. In Proceedings of the 8th International Congress on Catalysis, Berlin, 1984, Verlag-Chemie: Weinheim, 1984; Vol. III, p 649.
(5) Odenbrand, C. U. I.; Lundin, S. T.; Andersson, L. A. H. *Appl. Catal.* **1985**, *18*, 335.
(6) Bosch, H.; Janssen, F. J. J. G.; van den Kerkhof, F. M. G.; Odenziel, J.; van Ommen, J. G..; Ross, J. R. H. *Appl. Catal.* **1986**, *25*, 239.
(7) Siddiqi, A. A.; Tenini, J. W. *Hydrocarbon Process.* **1984**, *60*, 115.
(8) Murakami, Y.; Inomata, M.; Mori, K.; Ui, T.; Suzuki, K.; Miyamoto, A.; Hattori, T. *Preparation of Catalysts III*; Grange, P., Jacobs, J. P., Poncelet, G., Eds.; Elsevier: Amsterdam, 1983; p 1344.
(9) Haber, J.; Kozlowska, A.; Kozlowski, R. *J. Catal.* **1986**, *102*, 52.
(10) Roozeboom, F.; Mittelmeijer-Hazeleger, M.; Moulijn, J. A.; Medema, J.; de Beer, J. H. V.; Gellings, P. *J. Phys. Chem.* **1980**, *84*, 2783.
(11) Shikada, T.; Fujimoto, K.; Kunugi, T.; Tominaga, H.; Kaneko, S.; Kubo, Y. *Ind. Eng. Chem., Prod. Res. Dev.* **1981**, *20*, 91.
(12) Vogt, E. T. C.; de Boer, M.; van Dillen, A. J.; Geus, A. W. *Appl. Catal.* **1988**, *40*, 255.
(13) Reichman, M.; Bell, A. T. *Langmuir* **1987**, *3*, 111.
(14) Rajadhyaksha, R. A.; Hausinger, G.; Zeilinger, H.; Ramstetter, A.; Schmelz, H.; Knözinger, H. *Appl. Catal.* **1989**, *51*, 67.
(15) Baiker, A.; Dollenmeier, P.; Glinski, M.; Reller, A. *Appl. Catal.* **1987**, *35*, 365.
(16) Fernandez, A.; Leyrer, J.; González-Elipe. A. R.; Munuera, G.; Knözinger, H. *J. Catal.* **1988**, *112*, 489.
(17) Stranick, M. A.; Houalla, M.; Hercules, D. M. *J. Catal.* **1987**, *107*, 362.
(18) Matralis, H.; Fiasse, S.; Castillo, R.; Bastians, Ph.; Ruwet, M.; Grange, P.; Delmon, B. *Catal. Today* **1993**, *17*, 141.
(19) Liu, Z.; Tabora, J.; Davis, R. J. *J. Catal.* **1994**, *149*, 117.
(20) Miller, J. B.; Johnston, S. T.; Ko, E. I. *J. Catal.* **1994**, *150*, 311.
(21) Srinivasan, S.; Datye, A. K.; Hampden-Smith, M.; Wachs, I. E.; Deo, G.; Jehng, J. M.; Turek, A. M.; Peden, C. H. F. *J. Catal.* **1991**, *131*, 260.
(22) Yoldas, B. *J. Non-Cryst. Solids* **1980**, *81*, 38.
(23) Toba, T.; Mizukami, F.; Niwa, S.; Sano, T.; Maeda, K.; Annila, K.; Komppa, V. *J. Mol. Catal.* **1994**, *91*, 277.
(24) Doolin, P. K.; Alerasool, S.; Zalewski, D. J.; Hoffman, J. F. *Catal. Lett.* **1994**, *25*, 209.

0897-4756/95/2807-1342$09.00/0

on nonporous silica microspheres. The effect of the titanium content on the distribution of the titania layer has been investigated.

Experimental Section

Silica microspheres (Aerosil 200 from Degussa) with size ca. 13 nm diameter and surface area of 200 m^2/g were used as starting material. The TiO_2–SiO_2 materials were prepared by the homogenous precipitation method.[25] In this method, silica is suspended in deionized water to which an appropriate amount of $TiCl_3$ (Merck, 15% HCl solution) has been added while the suspension is vigorously stirred, ensuring a good homogeneity during the precipitation. Then the suspension is neutralized up to pH ca. 7 by slow addition of ammonium solution. The precipitate is repeatedly washed with deionized water and dried in air at 373 K for 12 h. The solid is then calcined at 773 K in air for 12 h. This procedure allows depositing hydrated Ti(III) oxide after thermal treatment to obtain dispersed TiO_2 on the silica surface. Four samples have been prepared, and they are referred to as xTiSi, where x denotes the titania loading in weight percent. For comparative purposes Degussa P25 Titania (85% anatase, 15% rutile) is used. The impurities level is <0.3% Al_2O_3, <0.3% HCl, <0.2% SiO_2, <0.01% Fe_2O_3, according to Degussa Technical Report.

The *specific surface areas* were calculated by the B.E.T. method from the nitrogen adsorption isotherms at 77 K measured in a Micromeritics ASAP-2000 Surface Analyzer. *Powder diffraction* patterns were recorded with a Phillips PW 1010 vertical diffractometer using nickel Cu Kα radiation. *Diffuse reflectance* UV–vis spectra were recorded on a Shimadzu UV-2100 spectrophotometer equipped with an integrating sphere using $BaSO_4$ as a reference. *Raman spectra* were obtained using a Brücker FT Raman instrument using a 1064 nm exciting line. Samples were placed in a stationary sample holder, under ambient conditions. The power measured at the sample was 20–40 mW. The radiation scattered from the sample was directed into a FT analyzer. *Lattice vibrations* were recorded with a Nicolet 5ZDX FTIR spectrophotometer using disks of the samples diluted (1:100) in KBr. The *acidity* properties were evaluated by ammonia adsorption on self-supported wafers (no KBr added) in an IR cell equipped with greaseless stopcocks and KBr windows. The samples were outgassed at 473 K and 10^{-4} Torr for 1 h and cooled to room temperature, before recording a background spectrum. Under this treatment no molecular water remains adsorbed on the surface[26] which could generate Brönsted acid sites. The samples were then exposed to 25 Torr of NH_3 at room temperature. The net spectrum of adsorbed ammonia is obtained by difference between the total and background spectra. *Photoelectron spectra* were recorded with a Fisons ESCALAB 200R spectrometer equipped with a Mg Kα X-ray source ($h\nu$ = 1253.6 eV) and a hemispherical electron analyzer. The powder samples were pressed into stainless steel cylinders and mounted on a long rod which allowed transfer from the preparation chamber to the analysis chamber. The residual pressure in the ion-pumped analysis chamber was maintained below 7×10^{-9} Torr during data acquisition. Energy regions of the photoelectrons were scanned at a pass energy of 20 eV. C_{1s}, O_{1s}, Si_{2p}, and Ti_{2p} peaks were recorded. The intensity was estimated by calculating the integral of each peak after subtraction of the S-shaped background and fitting to a curve mixed of Lorentzian and Gaussian lines of variable proportion.[27] Although surface charging was observed for all the samples, accurate binding energies (±0.2 eV) could be determined by charge reference to the C_{1s} or Si_{2p} peaks at 284.9 and 103.4 eV, respectively.

Results

Table 1 compiles the *specific surface areas* of the xTiSi materials. The area tends to decrease with increasing TiO_2 loading. However, for the highest loaded material, 48TiSi, the specific surface area increases again.

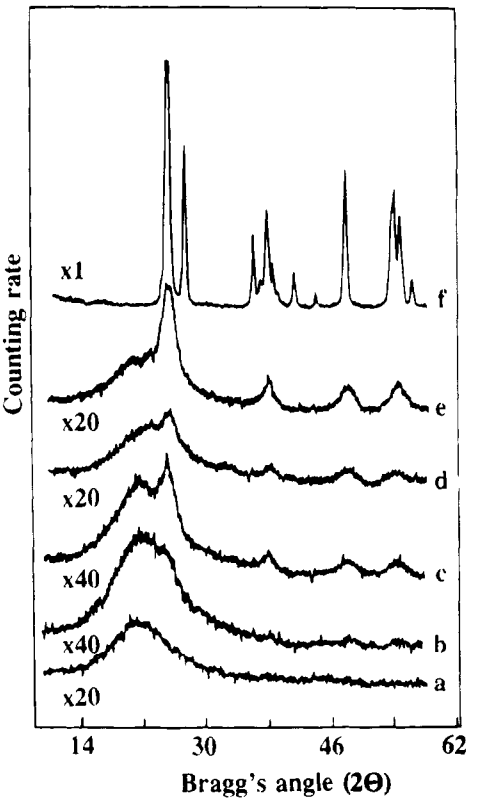

Figure 1. Powder X-ray diffraction patterns of TiO_2-coated silica microspheres with different TiO_2 loading: (a) pure SiO_2; (b) 8TiSi; (c) 16TiSi; (d) 32TiSi; (e) 48TiSi; (f) pure TiO_2.

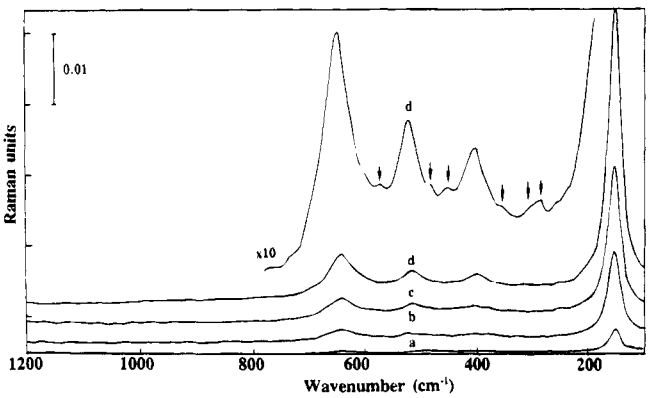

Figure 2. Raman spectra of TiO_2-coated silica samples: (a) 8TiSi; (b) 16TiSi; (c) 32TiSi; (d) 48TiSi. A expanded spectrum (d) of the 48TiSi sample is represented on the top. Arrows indicate bands of the brookite phase.

The XRD patterns of the samples are displayed in Figure 1. They show a broad peak characteristic of the X-ray amorphous silica matrix. The diffraction patterns of the 48TiSi sample and to a lesser extent of the 32TiSi and 16TiSi ones, showed superimposed broad diffraction peaks which can be indexed to anatase TiO_2. Line-broadening analysis for all these materials revealed that the crystal size of the titania anatase phase increases with increasing TiO_2 content. No large crystals of titania are expected to be present on 8TiSi material since no diffraction pattern is observed in this material.

Raman spectra of the xTiSi materials are presented in Figure 2. The samples that have undergone calcination at 773 K display four modes at 643, 515, 401, and

(25) Vogt, E. T. C.; Boot, A.; van Dillen, A. J.; Geus, J. W.; Janssen, F. J. J. G.; van den Kerkhof, F. M. G. *J. Catal.* **1988**, *114*, 313.
(26) Galán-Fereres, M.; Mariscal, R.; Alemany, L. J.; Fierro, J. L. G.; Anderson, J. A. *J. Chem. Soc., Faraday Trans.* **1994**, *90*, 3711.
(27) Shirley, D. A. *Phys. Rev.* **1972**, *35*, 4909.

152 cm^{-1} with an additional shoulder at 197 cm^{-1}. Anatase belongs to the space group D_{4h} 19 = 141/amd, with two formula units per unit cell. The factor group analysis predicts six Raman active modes ($A_{1g} + 2B_{1g} + 3E_g$) and three IR-active modes ($A_{2u} + 2E_u$). The Raman active modes for anatase have been assigned by Oshaka et al.[28] and the peaks at 643, 197, and 152 cm^{-1} are due to E_g symmetric modes, while that close to 515 cm^{-1} is due to the superimposition of two modes of $B1_g$ and $A1_g$ symmetry. Therefore, all fundamental vibrational modes are observed. The characteristic modes of anatase are present,[21,29] in accordance with the weak X-ray diffraction peaks associated with this phase. Some weak features are observed at ca. 549, 470, 440, 370, 294, 250, and 126 cm^{-1} characteristic of the brookite phase of titania (TiO_2(B), see expanded spectrum in Figure 2). The coexistence of anatase and TiO_2(B) on TiO_2-SiO_2 has already been reported.[13,30] However, in the present materials the contribution of brookite must be less than that previously found,[13,30] judging by the much weaker intensity of the brookite Raman bands and the absence of diffraction pattern characteristic of brookite in the XRD measurements. At low titania loadings the small size of the crystals causes a significant broadening of the XRD pattern, while the lowest titania loading contains titania in the anatase phase, but the particle size must be below 4 nm and hence does not produce a diffraction pattern. These small crystals are observed by Raman spectroscopy due to the higher sensitivity of the technique to small crystalline aggregates. The intensity of the Raman bands associated with anatase increase with titania loading. No bands characteristic of the rutile phase are observed. Formation of crystalline anatase on the silica substrate at loadings below monolayer capacity implies that the silica surface cannot stabilize a well-dispersed titania phase, which contrasts with the high degree of dispersion of titania incorporated into other oxides where a stronger interaction is developed. Other types of silicas also present a higher dispersion capacity.[21] The differences in the ability of silica to stabilize monolayer dispersion of titania is affected by the precursor and preparation procedures.[24,31]

Figure 3 exhibits the diffuse reflectance UV–vis spectra of *x*TiSi materials and the SiO_2 reference. Since SiO_2 is transparent in the explored range, light absorption must be due to the appearance of TiO_2 microstructures. The absorption spectra are blue-shifted with decreasing TiO_2 content, and they are dominated by edge relative to $O^{2-}Ti^{4+}$ charge transfer of TiO_2 anatase.

The binding energies of core electrons in *x*TiSi samples have been calculated from the photoelectron spectra.[25] The binding energies of $Ti_{2p3/2}$ and Si_{2p} peaks agree very well with the tabulated values for TiO_2 (anatase) and SiO_2[32] compounds. The O_{1s} profile was more complex as it could be fitted by two components: a first one close to 530.0 eV, whose proportion increased with Ti content,

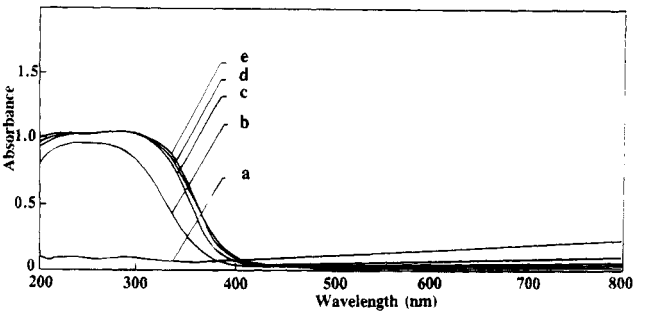

Figure 3. Diffuse reflectance spectra of TiO_2-coated silica samples: (a) SiO_2; (b) 8TiSi; (c) 16TiSi; (d) 32TiSi; (e) 48TiSi.

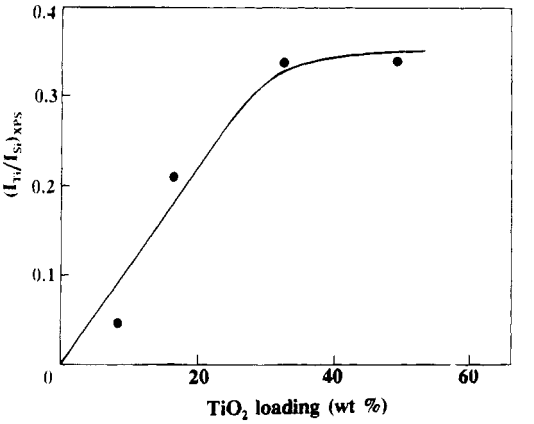

Figure 4. Dependence of the XPS Ti/Si intensity ratio with TiO_2 loading.

associated to lattice O^{2-} from TiO_2, and a second one at ca. 532.9 eV due to lattice O^{2-} from SiO_2. From the area of the $Ti_{2p3/2}$ and Si_{2p} peaks, the XPS Ti/Si intensity ratios were calculated. These ratios are given as a function of the titania loading in Figure 4. They increase progressively with increasing TiO_2 loading up to $x = 32$, and then they level off.

The infrared spectra of the titania–silica materials under dehydrated conditions in the silanol region show a sharp band at 3745 cm^{-1} characteristic of isolated silanol groups (Figure 5). Its intensity decreases with titania loading, reaching its lowest value for 32TiSi. At higher titania loading the silanol band is partly restored. As titania loading increases, a broad infrared feature at ca. 3650 cm^{-1} appears that makes difficult integration of the silanol IR band. For this reason the intensity of the IR band of the silanol group is used (Table 1). Additional information about the Ti–Si interface can be obtained from the framework vibrations, shown in Figure 6. The spectra display an extremely weak and broad absorption near 930 cm^{-1} and some features that are progressively modified by a broad absorption in the region below 800 cm^{-1}. The first peak has already been observed in the IR spectra of crystalline titanium–silicalite[33] and is assigned to a Ti–O–Si stretching mode. The same assignment has also been performed by Raman spectroscopy.[34] Since the IR band near 930 cm^{-1} is very weak, subtraction of the silica support spectrum has been performed on samples 16TiSi, 32TiSi, and 48TiSi (inset in Figure 6). An

(28) Oshaka, T.; Izumi, F.; Fujiki, Y. *J. Raman Spectrosc.* **1978**, *7*, 321.
(29) Wachs, I. E.; Hardcastle, F. D. *Proc. 9th. Int. Congr. Catal.* **1988**, *3*, 1449.
(30) Reichmann, M. G.; Bell, A. T. *Appl. Catal.* **1987**, *32*, 315.
(31) Srinivasan, S.; Datye, A. K.; Smith, M. H.; Peden, C. H. F. *J. Catal.* **1994**, *145*, 565.
(32) *Practical Surface Analysis:Auger and X-ray Photoelectron Spectroscopy*; Briggs, D., Seah, M. P., Eds.; John Wiley & Sons: Chichester, 1990.
(33) Walther, K. L.; Wokaum, A.; Handy, B. E.; Baiker,A. *J. Non-Cryst. Solids* **1991**, *134*, 47.
(34) Deo, G.; Turek, A. M.; Wachs, I. E.; Huybrechts, D. R. L.; Jacobs, P. A. *Zeolites* **1993**, *13*, 365.

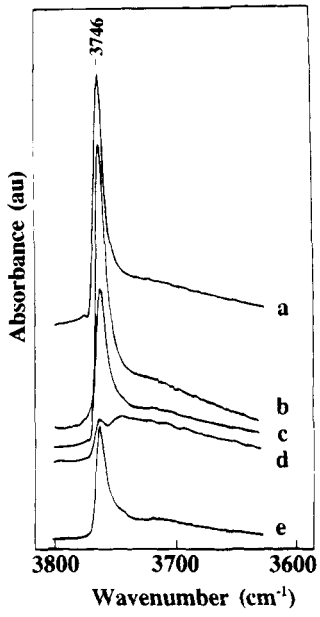

Figure 5. IR spectra in the OH stretching region for samples (a) pure SiO_2; (b) 8TiSi; (c) 16TiSi; (d) 32TiSi; (e) 48TiSi.

Table 1. Properties of the TiO_2–SiO_2 Materials

label	TiO_2[a] (wt %)	S_{BET} (m^2/g)	intensity silanol
Si	0	200	
8TiSi	8.0	208	489
16TiSi	16.0	176	129
32TiSi	32.0	169	3
48TiSi	48.0	213	210
Ti	100	50	

[a] Nominal content.

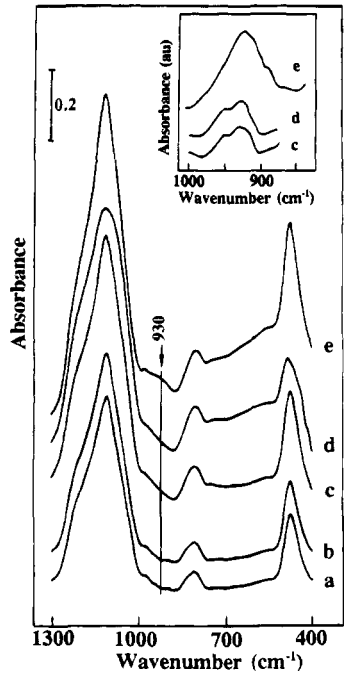

Figure 6. Framework vibrations of the TiSi samplesin KBr: (a) pure SiO_2; (b) 8TiSi; (c) 16TiSi; (d) 32TiSi; (e) 48TiSi. Inset corresponds to net spectra c–e after subtraction of the silica support.

additional broad band, having a shoulder near 750 cm^{-1}, and the main band near 450 cm^{-1} can be distinguished. All of these features correspond to the anatase phase. These spectroscopic data confirm that the samples contain anatase and, additionally, that Ti–O–Si bonds

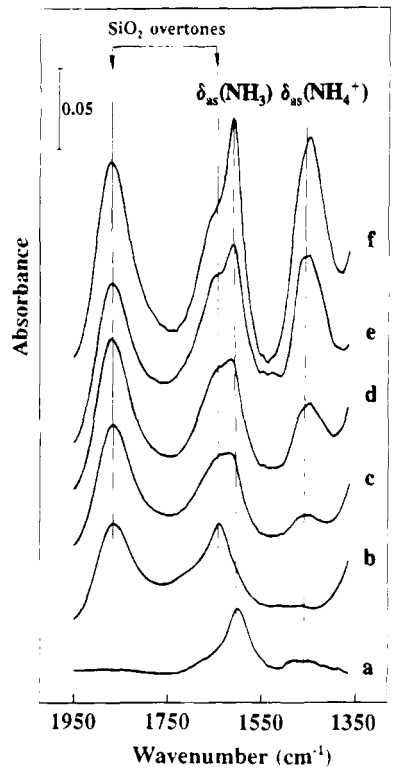

Figure 7. Transmission FTIR spectra of ammonia adsorbed at room temperature on self-supported samples: (a) pure TiO_2; (b) pure SiO_2; (c) 8TiSi; (d) 16TiSi; (e) 32TiSi; (f) 48TiSi.

may exist in the structure. The progressive consumption of the silica hydroxyl groups (Table 1) with increasing titania loading up to 32TiSi must be associated with the formation of the Ti–O–Si bonds.

The acidic properties are examined by the vibrational modes of adsorbed ammonia on dehydrated self-supported wafers and the study of the stability of the surface species formed upon adsorption of ammonia. IR spectra of the adsorption of ammonia is presented in Figure 7. The presence of a variety of surface centers can be derived from the analysis of the vibrational spectra of adsorbed ammonia. No clean absorption bands associated to ammonia species are detected for ammonia adsorption on silica. For the sake of clarity, the two silica overtones have been marked by arrows in Figure 7. Conversely, pure anatase sample displays a strong band at 1596 cm^{-1} attributed to the asymmetric deformation mode of coordinatively bonded ammonia on Lewis acid sites, i.e., Ti^{4+} ions. For all the xTiSi samples, the spectra of ammonia showed a band near 1600 cm^{-1}, attributed to the asymmetric deformation of coordinatively bonded ammonia. Its symmetric deformation counterpart cannot be observed since it would appear at ca. 1150 cm^{-1} beyond the energy "cutoff" of the signal for these samples near 1300 cm^{-1}. Another absorption at 1450 cm^{-1}, associated with the asymmetric deformation of ammonium ion (NH_4^+), reveals the presence of small amounts of protonic (Brönsted) sites on their surface.

A study of the thermal stability of adsorbed ammonia after outgassing at different temperatures is presented in Figure 8. In all of the samples, the spectra of the corresponding evacuated sample has been subtracted to better evaluate the different acid sites. The IR spectra of adsorbed ammonia on 8TiSi, 32TiSi, and reference Degussa P-25 titania samples after outgassing

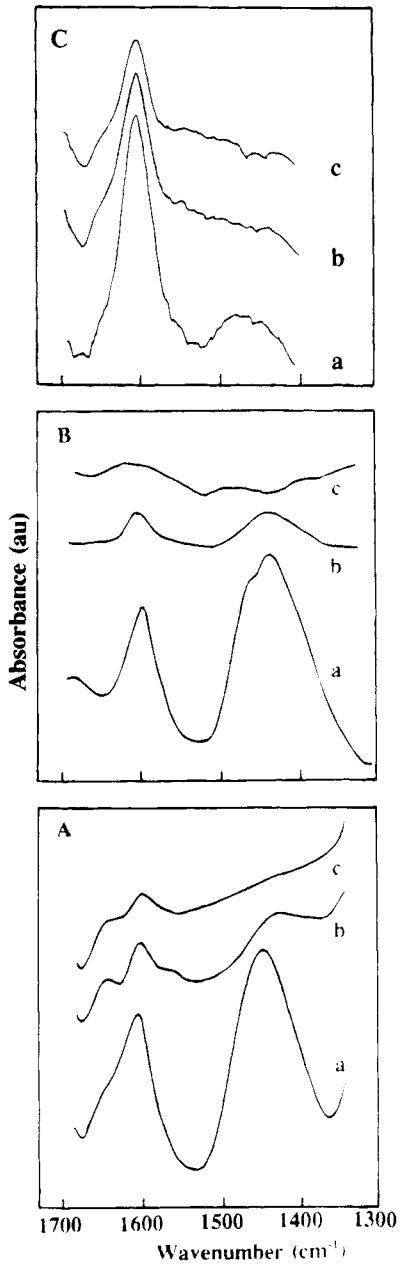

Figure 8. Transmission FTIR spectra of adsorbed ammonia after evacuation at (a) 298 K; (b) 473 K; (c) 573 K. (A) 8TiSi; (B) 32TiSi; (C) Degussa P-25 Titania.

at 298, 473, and 573 K are displayed in Figure 8a–c, respectively. It can be seen that the intensity of the band assigned to NH_4^+ species is greater than the band for adsorbed NH_3 on both *x*TiSi samples outgassed at ambient temperature, but the intensities are equivalent following outgassing at 473 K. A weak IR band of adsorbed NH_4^+ is observed on Degussa P-25 titania. Since no Brönsted acid sites are observed on pure titania,[35] this weak feature must be related to Al and Fe impurities present on the titania used.[34] Finally, the sample outgassed at 573 K display only the band assigned to coordinatively adsorbed ammonia. A similar band is observed for NH_3 adsorption on the Degussa P25 TiO_2 reference. It can be inferred that a small proportion of very strong Lewis acid sites associated with the titania are present on both materials which still hold ammonia at this temperature, whereas the NH_4^+ molecules adsorbed on Brönsted sites are less stable.

(35) Tanaka, K.; White, J. M. *J. Phys. Chem.* **1982**, *86*, 4708.

Discussion

The existence of crystalline TiO_2 as anatase on the highest loaded TiSi materials is clearly indicated by the XRD and FT Raman measurements. A significant decrease in the crystal size is noted by the line broadening observed in diffraction patterns upon decreasing the titanium loading. On the lowest loaded sample (8TiSi) no diffraction pattern can be observed; however, the presence of a Raman band at 144 cm^{-1} and some features at ca. 400, 520, and 643 cm^{-1} clearly indicate the existence of small anatase crystallites. These crystallites must be smaller than 4 nm since they are not large enough to generate diffraction pattern. The blue shift observed in UV–vis spectra supports the presence of very small titania domains, and suggests the presence of surface tetrahedral titania species.[19,36] Some authors have reported the existence of some dispersed surface tetrahedral titania species on silica[37] characterized by laser Raman spectroscopy by features at Raman shifts ca. 1060, 920, and 788 cm^{-1}, related to Ti–O–Si vibrations[34,37] and by XANES.[34,38] Unfortunately FT Raman spectroscopy has a lower sensitivity to dispersed surface species and no direct evidence can be given for their existence.

Diffuse reflectance UV–vis spectroscopy provides additional information on the nature of the titanium sites. Absorption spectra are very close to that of pure bulk titania. No reduced titania sites are indicated for the TiSi materials since no significant absorption is recorded in the visible region, characteristic of d–d transitions. The significant shift in the profiles to higher energies observed on the 8TiSi sample compared with higher loaded samples has been attributed to small sized titania particles,[36,38,39] which is in agreement with observations by XRD and FT Raman. The changes observed with the titania loading in UV–vis spectra are also due to a change in the coordination sphere of titanium since the tetrahedral Ti^{4+} species absorb at higher energies.[19] This is an additional cause for the blue-shift in the DRS–UV–vis spectra of the 8TiSi since the structure of the silica support determines the arrangement of the titanium oxide species anchored on it by the Ti–O–Si bonds.[38] This interaction produces tetrahedrally coordinated titanium sites.[38]

The surface distribution of the small titania crystallites appears to be quite homogeneous over the silica surface for loadings up to 32% TiO_2, as indicated by the relative titanium-to-silicon XPS intensities. The progressive elimination of the silica support hydroxyl groups in this region (Table 1, Figures 5 and 9) clearly indicates that titanium oxide species anchor to the silica hydroxyl groups in this range of titania loading. Since titania–silica catalysts were prepared using hydroxylated silica, a more uniform mixing of the oxides is expected compared with a dehydroxylated silica which would favor nucleation of the titania,[20] thus yielding islands of titania on the silica support. Previous

(36) Henglein, A. *Chem. Rev.* **1989**, *89*, 1861.
(37) Jehng, J.-M.; Wachs, I. E. *Catal. Lett.* **1992**, *13*, 9.
(38) Liu, Z; Davis, R. J. *J. Phys. Chem.* **1994**, *98*, 1253.
(39) Fernández, A.; Leyrer, J.; González-Elipe, A. R.; Munuera, G.; Knözinger, H. J. *J. Catal* **1988**, *112*, 489.

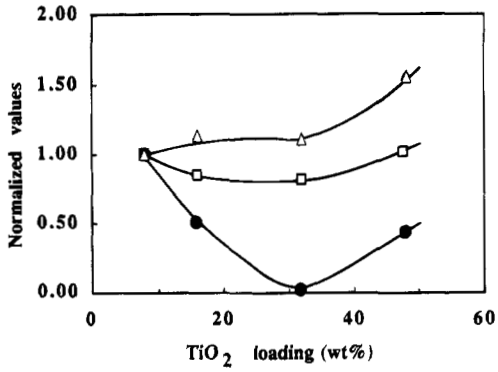

Figure 9. Evolution of the relative adsorbed NH_3/NH_4^+ (triangle), available silica hydroxyl groups (dot), and specific surface area (square) with TiO_2 loading. For comparison, all the values of the different series have been normalized to the initial value in each series.

research shows that isolated silanol groups play an important role in dispersing oxides. Roark et al.[40] show that isolated silanol groups assist in spreading supported molybdena on silica upon dehydration. FTIR spectroscopy shows a consumption of silanol groups upon dehydration of silica-supported molybdena.[40] The process is reversible, and after hydration the isolated silanol groups are restored. This behavior upon dehydration has not been observed for TiO_2–SiO_2 materials[31] which has led to some doubts on the role of silanol groups in the dispersion of titania.[31] A distinction between silica-supported molybdenum oxide and titanium oxide should be made. Under atmospheric conditions, silica-supported molybdenum oxide species hydrate forming solvated heptamolybdate species. Upon dehydration they become unstable and break, spreading on the silica[41,42] at the expense of silanol groups.[40] However, alumina-supported titania has been shown to be insensitive to this hydration/dehydration phenomena.[43] TiO_2–SiO_2 show some modifications of titania species upon exposure of dehydrated samples to ambient conditions[34] but do not appear to fully hydrolyze bonds with the silica support. Consequently, no change in the silanol population is expected to take place upon dehydration. However, the progressive consumption of isolated silanol groups with increasing titania loading up to 32TiSi (Table 1, Figures 5 and 9) clearly supports the role of isolated silanol groups in anchoring titanium oxide. The same behavior is observed on silica-supported molybdenum oxide when molybdenum loading is increased.[44] Therefore, the interaction with silanol groups may generate Ti–O–Si bonds in the oxide interface. A detailed analysis of the infrared spectra in the framework vibration region presented in Figure 6 shows a feature at ca. 930 cm^{-1} which has been attributed to Ti–O–Si bonds at the TiO_2–SiO_2 interface.[45] A similar band at ca. 930 cm^{-1} observed by laser Raman spectroscopy has been related to Ti–O–Si vibrations.[34,37] Due to the larger amounts of titania and silica oxides compared to the TiO_2–SiO_2 interface, the presence of the bands at 930 cm^{-1} characteristic of Ti–O–Si is not much evident. Even when subtraction spectra (inset in Figure 6) make clear its existence no quantitative discussion can be afforded. The remarkable consumption of silica hydroxyl groups reported above and studies of the TiO_2–SiO_2 system by ^{29}Si NMR provide evidence for the existence of Ti–O–Si bonds.[33] No significant differences are observed between the XPS titanium to silicon ratio of 32TiSi and 48TiSi. However a significant sharpening for the anatase diffraction pattern is observed in the XRD diffractogram and all the Raman bands characteristic of anatase can clearly be observed on 48TiSi sample. Consequently, larger titania (anatase) crystals are formed at highest titania loadings. In addition, the FTIR spectra show a remarkable relative increase in the amount of silanol groups (Table 1, Figures 5 and 9). Consequently, at this highest loading the two oxides tend to segregate, thus forming larger crystals with a lesser interaction with the silica. As a consequence, the larger amount of titania is less evident from XPS due to the poorer coverage of the silica and larger size of the anatase crystals. The poor coverage of the silica by titania on 48TiSi sample must account for the increase in the specific surface area.

Infrared measurements show no acid sites upon adsorption of ammonia on silica. Titania, conversely, is characterized by Lewis acid sites, as shown by the IR band at 1596 cm^{-1}, associated with octahedral surface titanium sites in the anatase crystal. The weak Brönsted acidity observed on Degussa P-25 titania is most likely related to impurities.[34,49] However, TiO_2–SiO_2 materials present a new kind of acid site (Brönsted acidity) which is not observed on either of the constituting pure oxides (Figure 8a). Therefore, the new acidity must originate from some new type of site. Characterization of the TiSi materials reveals the existence of Ti–O–Si bonds. However, it has been reported that Ti–O–Si bonds do not yield Brönsted acidity on titania–silicalites or titania–silica at low titania loadings.[19,34] Titanium integrates in silica and silicalite matrix by isomorphic substitution. Under these conditions no charge unbalance is expected, as suggested by Tanabe's theory.[46–48] As titanium loading increases, the Brönsted to Lewis acid sites ratio remains essentially constant until silanol groups consumption (Figure 9). Small domains of titania (anatase) are present. Titanium has an octahedral coordination in titania (anatase). Titania domains must coordinate to the silica support by reaction with surface silanol groups. This new scenario provides octahedral titania sites integrating into tetrahedral silica matrix generating nonbalanced oxygen atoms. The charge unbalance requires acidic bridging hydroxyl groups that must account for the Brönsted acidity.[46,47] Additional acidity due to surface sites on titania particles should not be ruled out. Indeed, a small fraction of silica could be dissolved in the acidic

(40) Roark, R. D.; Kohler, S. D.; Ekerdt, J. G. *Catal. Lett.* **1992**, *16*, 71.
(41) de Boer, M.; van Dillen, A. J.; Konigsberger, D. C.; Vuurman, M. A.; Wachs, I. E.; Geuss, J. G. *Catal. Lett.* **1991**, *11*, 227.
(42) Williams, C. C.; Ekerdt, J. G.; Jehng, J. M.; Hardcastle, F. D.; Turek, A. M.; and Wachs, I. E. *J. Phys. Chem.* **1991**, *95*, 8781.
(43) Vuurman, M. A.; Wachs, I. E. *J. Phys. Chem.* **1992**, *96*, 5008.
(44) Liu, T.-Ch.; Forissier, M.; Goudurier, M.; Vèdrine, J. C. *J. Chem. Soc., Faraday Trans. 1* **1989**, *85*, 1607.
(45) Odenbrand, C. V. I.; Andersson, S. L. T.; Andersson, L. A. H.; Brandin, J. G. M.; Busca, G. *J. Catal.* **1990**, *125*, 541.
(46) Tanabe, K. In *New Solid Acids and Bases*; Tanabe, K., Misono, M., Ono, Y., Hattori, H., Eds.; Kodansha and Elsevier: Tokyo; Vol. 51, Chapter 3.
(47) Seiyama, T. In *Metal Oxides and Their Catalytic Actions*; Kodansha: Tokyo, 1978; p 41.
(48) Tanabe, K. *Catal. Sci. Technol.* **1981**, *2*.
(49) Solar, J. P.; Basu, P.; Shatlock, M. P. *Catal. Today* **1992**, *14*, 211.

medium used to make Ti–Si materials and locate on titania particles. It should also result in charge unbalance, thus generating Brönsted acid sites. However, most of Brönsted acid sites appear to originate from the charge unbalance associated to titania–silica interface.

The lowest titania loaded sample (8TiSi) has very ill-defined titania aggregates as suggested by weak Raman features. The significant shift to higher energies observed on UV–vis spectra for 8TiSi strongly supports the existence of extremely small titania domains and/or tetrahedral titanium sites integrated into the titania structure.[19] The linear increase of Ti/Si XPS atomic ratio in this loading range clearly supports the existence of a highly dispersed titania phase. Consequently, very few Brönsted acid sites are expected on 8TiSi. Aggregation of titania phase at higher titania loadings as shown by Ti/Si XPS atomic ratio trend, FT Raman features, UV–vis spectroscopy, and XRD patterns. The larger size of octahedral titania (anatase) phase in contact with silica support generates charge unbalance on titania sites at the TiO_2–SiO_2 interphase. However, for the highest loaded 48TiSi material, nucleation of titania must predominate versus precipitation on silica. Silanol consumption is minimized due to the resulting phase segregation, and Brönsted acidity decreases accordingly (Figure 9). In addition, segregation of the two oxides significantly reduces coverage of the silica, thus restoring part of its surface area.

Further investigation of the thermal stability of adsorbed ammonia reveals the presence of some type of strong Lewis acid sites which are low in number (Figure 8b) compared with the bulk titania P-25. The strong Lewis acidity is already present on a reference titania Degussa P-25 (anatase and rutile are present), where no titania–silica interface can be formed. Consequently, the strong Lewis acid sites are already present on the titania phase, and supporting on silica does not appear to generate significant additional Lewis acidity.

Conclusions

The titanium oxide incorporated on silica remains as small crystals covering the silica surface thus decreasing the specific surface area of the materials. The presence of TiO_2 on silica yields Brönsted acidity and Lewis acidity. At higher titania loadings larger titania (anatase) phase provides a matrix effect which grants an octahedral environment to titanium atoms coordinating to the silica substrate. Brönsted acidity appears to be associated with the interface between silica and octahedral titania, characterized by Si–O–Ti bonds. The strong Lewis acidity observed on the titania–silica materials is already present for bulk titania. Brönsted acidity appears to be due to the Si–O–Ti bonds formed at the interface between silica and bulk octahedral titania, as indicated by silanol consumption. At high titania loadings (48TiSi) both oxides tend to segregate thus decreasing the TiO_2–SiO_2 interface and Brönsted acidity decreases markedly.

Acknowledgment. This work was supported by European Union research programme EV5V-CT92-0234. L.J.A. acknowledges the Spanish Ministry of Education and Science for a postdoctoral contract. M.A.B. acknowledges the European Union for a postdoctoral grant JOU2-CT93-0354.

CM9500465